

Eta meson rescattering effects in the $p + {}^6\text{Li} \rightarrow \eta + {}^7\text{Be}$ reaction near threshold

N. J. Upadhyay¹, N. G. Kelkar² and B. K. Jain¹

¹ *Dept. of Physics, University of Mumbai, Kalina, Mumbai, India*

² *Dept. de Fisica, Univ. de los Andes,*

Cra. 1E, No. 18A-10, Bogota, Colombia

Abstract

The $p + {}^6\text{Li} \rightarrow \eta + {}^7\text{Be}$ reaction has been investigated with an emphasis on the η meson and ${}^7\text{Be}$ interaction in the final state. Considering the ${}^6\text{Li}$ and ${}^7\text{Be}$ nuclei to be α -d and α - ${}^3\text{He}$ clusters respectively, the reaction is modelled to proceed via the $p + d[\alpha] \rightarrow {}^3\text{He}[\alpha] + \eta$ reaction with the α remaining a spectator. The η meson interacts with ${}^7\text{Be}$ via multiple scatterings on the ${}^3\text{He}$ and α clusters inside ${}^7\text{Be}$. The individual η - ${}^3\text{He}$ and η - α scatterings are evaluated using few body equations for the η - ${}^3\text{N}$ and η - ${}^4\text{N}$ systems with a coupled channel η - N interaction as an input. Calculations including four low-lying states of ${}^7\text{Be}$ lead to a double hump structure in the total cross section corresponding to the $L = 1 (J = (1/2)^-, (3/2)^-)$ and $L = 3 (J = (5/2)^-, (7/2)^-)$ angular momentum states. The humps arise due to the off-shell rescattering of the η meson on the ${}^7\text{Be}$ nucleus in the final state.

PACS numbers: 25.40.Ve, 21.85.+d, 25.10.+s

I. ETA MESON INTERACTIONS WITH LIGHT NUCLEI

The past few years have seen extensive investigations of the η meson producing reactions at close to threshold energies. The experiments are aimed either at directly searching [1] for the possible existence of eta-mesic nuclei as a result of the strong attractive nature of the η -N interaction [2] or studying the final state eta-nuclear interaction to eventually conclude on the existence of eta-mesic nuclear states [3, 4]. A common feature of the data on η production near threshold is the strong deviation of the cross sections from phase space. It can be understood as a manifestation of the strong attractive η -N interaction (arising basically due to the proximity of the η -N threshold to the S_{11} resonance $N^*(1535)$). Experiments on η production have been performed in nucleon-nucleon collisions and have been extended to proton-deuteron and deuteron-deuteron collisions too [5]. Though the focus of reactions such as the $p + d \rightarrow p + d + \eta$ and $p + d \rightarrow {}^3\text{He} + \eta$ is on investigating possibilities of bound states of eta mesons and 2 - 3 nucleon systems, theoretical studies of the reaction mechanism revealed interesting features too [6]. In the p-d collisions, the production near threshold is found to be dominated by a two-step mechanism where the large momentum transfer in producing the η meson is shared by three nucleons. These findings naturally led to the curiosity of what happens when the η interacts with more than three or four nucleons in the final nucleus. With this motivation, measurements of the $p + {}^6\text{Li} \rightarrow \eta + {}^7\text{Be}$ reaction were carried out by the Turin group in 1993 [7] at an incident energy of 683 MeV. A theoretical study of this reaction along with others of the type, $a + {}^6\text{Li} \rightarrow b + {}^7\text{Be}$ and $a + {}^6\text{Li} \rightarrow b + {}^7\text{Li}$ was performed in [8]. Part of the emphasis of this work was on obtaining the right form factors for ${}^7\text{Li}$ (and ${}^7\text{Be}$) and the interactions of the mesons with the nuclei in the final states were neglected. The interest in the $p + {}^6\text{Li} \rightarrow \eta + {}^7\text{Be}$ reaction revived once again by the recent proposal of studying this reaction at COSY, Jülich, at an incident energy of 673 MeV [9].

Having performed detailed theoretical studies of the $p + d \rightarrow p + d + \eta$ and $p + d \rightarrow {}^3\text{He} + \eta$ reactions [6] and the η meson interactions with the deuteron, ${}^3\text{He}$ and ${}^4\text{He}$ nuclei [3], we now develop a model to study the interaction of η mesons with a ${}^3\text{He}$ - ${}^4\text{He}$ cluster, namely, the ${}^7\text{Be}$ nucleus. The η - ${}^7\text{Be}$ interaction is then incorporated in a theoretical calculation of cross sections for the $p + {}^6\text{Li} \rightarrow \eta + {}^7\text{Be}$ reaction, with four possible low-lying states of the ${}^7\text{Be}$ nucleus. An analysis of its effects on the $p + {}^6\text{Li} \rightarrow \eta + {}^7\text{Be}$ cross sections presented

here, should be useful in motivating further experimental studies of this reaction.

II. CLUSTER MODEL APPROACH

Based on literature which supports considering the ${}^7\text{Be}$ nucleus as a bound state of an alpha (${}^4\text{He}$) and ${}^3\text{He}$ [10], we model the η - ${}^7\text{Be}$ final state interaction in the form of a three body problem of the η - ${}^3\text{He}$ - ${}^4\text{He}$ interaction. Regarding the ${}^6\text{Li}$ too as a cluster of an alpha and a deuteron [11], the $p + {}^6\text{Li} \rightarrow \eta + {}^7\text{Be}$ reaction is considered to proceed through the $p + d \rightarrow {}^3\text{He} + \eta$ reaction with the α remaining a spectator. Besides, the present work focuses on the low energy region of η production where (a) the $p + d \rightarrow {}^3\text{He} + \eta$ production amplitude is large (i.e. the p and d interact strongly to produce an η) and (b) the cluster picture of low lying levels of ${}^7\text{Be}$ and ${}^6\text{Li}$ is reasonably good. There exists in principle, the possibility of considering the deuteron as a spectator. However, a reaction of the type $p + \alpha \rightarrow {}^5\text{Li} + \eta$ followed by the combination of ${}^5\text{Li}$ and a deuteron to form the ${}^7\text{Be}$ nucleus, does not agree with the cluster model approach here (since ${}^7\text{Be}$ is hardly known to be a cluster of $d + {}^5\text{Li}$, where ${}^5\text{Li}$ is in fact unstable). The possibility of an intermediate $p + \alpha \rightarrow p + \alpha + \eta$ reaction, with further steps of the final state p from this reaction combining with the spectator deuteron, i.e., $p + d$ forming a ${}^3\text{He}$ which eventually combines with the final state α (from the above reaction) to form ${}^7\text{Be}$ still remains. However, this is not a practical option with no information available on the $p + \alpha \rightarrow p + \alpha + \eta$ reaction.

A. Elastic scattering of eta mesons on ${}^7\text{Be}$

As mentioned above, we consider the ${}^7\text{Be}$ nucleus as a two body system made up of a ${}^3\text{He}$ and ${}^4\text{He}$ nucleus and construct an elastic transition matrix for the three body problem of an η meson, ${}^3\text{He}$ nucleus and an α (${}^4\text{He}$). The individual scattering of the η meson on ${}^3\text{He}$ and α is evaluated using the t -matrices constructed earlier by the present authors [3]. These t -matrices are numerically evaluated using few body equations and include the off-shell rescattering of the η on the nucleons inside ${}^3\text{He}$ and ${}^4\text{He}$. The η - ${}^3\text{He}$ t -matrix is tested to reproduce the $p + d \rightarrow {}^3\text{He} + \eta$ cross section reasonably well [6].

To formulate the three body problem of the η - ${}^3\text{He}$ - ${}^4\text{He}$ interaction, let us define \vec{r}_1 and \vec{r}_2 to be the coordinates of the ${}^3\text{He}$ and ${}^4\text{He}$ nuclei respectively, with respect to the mass-

7 centre of mass system. Defining the internal Jacobi coordinate of the relative distance between the ${}^3\text{He}$ and ${}^4\text{He}$ nuclei as \vec{x} , one can see that $\vec{r}_1 = a_1\vec{x}$ and $\vec{r}_2 = a_2\vec{x}$ with $a_1 = 4/7$ and $a_2 = -3/7$. The η - ${}^7\text{Be}$ t-matrix is then written as,

$$T_{\eta-{}^7\text{Be}}(\vec{k}', \vec{k}, z) = \int d^3x |\Psi_L^7(\vec{x})|^2 [T_1(\vec{k}', \vec{k}, a_1\vec{x}, z) + T_2(\vec{k}', \vec{k}, a_2\vec{x}, z)] \quad (1)$$

where $T_1(\vec{k}', \vec{k}, a_1\vec{x}, z)$ and $T_2(\vec{k}', \vec{k}, a_2\vec{x}, z)$ are the medium modified t-matrices for the off-shell η scattering on the bound ${}^3\text{He}$ and ${}^4\text{He}$ respectively. $\Psi_L^7(x)$ represents the cluster wave function of ${}^7\text{Be}$ with angular momentum L and $z = E - |\varepsilon_0| + i\epsilon$, where, E is the total η -nucleus energy in the centre of mass and ε_0 is the energy required for the break up of ${}^7\text{Be} \rightarrow {}^3\text{He} + {}^4\text{He}$. The in-medium η - ${}^3\text{He}$ and η - ${}^4\text{He}$ t-matrices are written using a Faddeev type decomposition [12], namely,

$$T_i(\vec{k}', \vec{k}, a_i\vec{x}, z) = t_i(\vec{k}', \vec{k}, a_i\vec{x}, z) + \int \frac{dk''}{(2\pi)^3} \frac{t_i(\vec{k}', \vec{k}'', a_i\vec{x}, z)}{z - k''^2/2\mu} \sum_{j \neq i} T_j(\vec{k}'', \vec{k}, a_j\vec{x}, z), \quad (2)$$

where $i = 1, 2$ and the indices 1 and 2 correspond to the ${}^3\text{He}$ and ${}^4\text{He}$ t-matrices respectively. The t_i 's represent the single scattering terms and are the matrices for purely elastic η - ${}^3\text{He}$ and η - ${}^4\text{He}$ scattering. They have the form,

$$t_i(\vec{k}', \vec{k}; \vec{r}_i; z) = t_i(k', k; z) \exp[i(\vec{k} - \vec{k}') \cdot \vec{r}_i], \quad (3)$$

with $\vec{r}_i = a_i\vec{x}$ and $i = 1, 2$ as mentioned above. At the low energies considered here, the η -N interaction is dominated by the S_{11} resonance $N^*(1535)$ and hence we perform a partial wave expansion and retain only s -waves, which reduces (2) to the following two equations for η - ${}^3\text{He}$ (T_1) and η - ${}^4\text{He}$ (T_2):

$$T_1(k', k, a_1x, z) = t_1(k', k, a_1x, z) + \int \frac{dk''}{2\pi^2} k''^2 \frac{t_1(k', k'', a_1x, z)}{z - k''^2/2\mu} T_2(k'', k, a_2x, z) \quad (4)$$

$$T_2(k', k, a_2x, z) = t_2(k', k, a_2x, z) + \int \frac{dk''}{2\pi^2} k''^2 \frac{t_2(k', k'', a_2x, z)}{z - k''^2/2\mu} T_1(k'', k, a_1x, z), \quad (5)$$

where $t_i(\vec{k}', \vec{k}; \vec{r}_i; z)$ in Eq. (3) has reduced to $t_i(k', k, a_ix, z)$ written in terms of the spherical Bessel functions $j_0(a_ixk)$ and $j_0(a_ixk')$. Replacing the equation for T_2 in T_1 , we obtain a recursive relation for T_1 as follows,

$$T_1(k', k, a_1x, z) = t_1(k', k, a_1x, z) + \int \frac{dk''}{2\pi^2} k''^2 \frac{t_1(k', k'', a_1x, z)}{z - k''^2/2\mu} t_2(k'', k, a_2x, z) \quad (6)$$

$$+ \int \int \frac{dk'' d\tilde{k}}{4\pi^4} k''^2 \tilde{k}^2 \frac{t_1(k', k'', a_1x, z) t_2(k'', \tilde{k}, a_2x, z) T_1(\tilde{k}, k, a_1x, z)}{(z - k''^2/2\mu)(z - \tilde{k}^2/2\mu)}.$$

Once T_1 is evaluated from (6), it can be replaced into the equation for T_2 and the two can be substituted in (1) to evaluate the η - ^7Be t-matrix. Thus (1) is evaluated retaining only s -waves in T_1 and T_2 . T_1 is evaluated numerically using the η - ^3He and η - ^4He t-matrices, t_1 and t_2 respectively, as inputs. t_1 and t_2 are themselves evaluated numerically using few body equations and an input coupled channel η - N t-matrix. Details of this formalism can be found in [3]. The two models of the elementary ηN t-matrix used here will be discussed in the next subsection.

1. Models of elementary η -nucleon scattering

The coupled channel η - N t-matrix which is required for the evaluation of the η - ^3He and η - ^4He t-matrices, t_1 and t_2 , is taken from two different models available in literature. In [13], a transition matrix including the πN and ηN channels with the $N^*(1535)$ resonance playing a dominant role was constructed. It consisted of the meson - N^* vertices and the N^* propagator as given below:

$$t_{\eta N \rightarrow \eta N}(k', k; z) = \frac{g_{N^*} \beta^2}{(k'^2 + \beta^2)} \tau_{N^*}(z) \frac{g_{N^*} \beta^2}{(k^2 + \beta^2)} \quad (7)$$

with, $\tau_{N^*}(z) = (z - M_0 - \Sigma_\pi(z) - \Sigma_\eta(z) + i\epsilon)^{-1}$, where $\Sigma_\alpha(z)$ ($\alpha = \pi, \eta$) are the self energy contributions from the πN and ηN loops. In [13] elastic and inelastic η -deuteron scattering as well as η photoproduction on the deuteron was studied using this ηN model. We shall use two parameter sets available, one which leads to a scattering length of $a_{\eta N} = (0.75, 0.27)$ fm and another which leads to $a_{\eta N} = (0.88, 0.41)$ fm. We shall refer to this model henceforth as Model A.

Model B used in the present work is taken from [14]. The t-matrix for $\eta N \rightarrow \eta N$ is written in a separable form as,

$$t_{\eta N \rightarrow \eta N}(k', k; z) = v(k') t_{\eta\eta}(E) v(k), \quad (8)$$

where the on-shell part, $t_{\eta\eta}(E)$, is described in an effective range approximation as,

$$t_{\eta\eta}(E)^{-1} + i q v(q)^2 = \frac{1}{a} + \frac{r_0}{2} q^2 + s q^4. \quad (9)$$

The off-shell form factors have the form, $v(k) = 1/(1 + k^2 \Lambda^2)$, where Λ is the length parameter in this model. The parameter sets in this model are obtained from a fit to the

$\pi N \rightarrow \pi N$, $\pi N \rightarrow \eta N$, $\gamma N \rightarrow \pi N$ and $\gamma N \rightarrow \eta N$ data. The parameters required in Eqs. (8) and (9) above can be found in [14]. We choose four parameter sets with ηN scattering lengths of (0.88,0.25) fm, (0.77, 0.25) fm, (0.51,0.26) fm and (0.4, 0.3) fm.

2. Kinematics of the many body problem

The choice of kinematic variables in a multiple scattering formalism where the many body scattering matrix is written in terms of a two body matrix is not unique in literature. The two most commonly used approaches are (i) the fixed scatterer approximation (FSA) and (ii) the on-energy shell impulse approximation (OEI) [15] (related to yet another approach, namely, the fixed impulse approximation (FIA) [16]). The difference between these approaches (which becomes important at intermediate and high energies) lies in the fact that in the FSA, the struck nucleon is assumed to recoil with the target as a whole, while in the OEI, it recoils freely. This means that in the FSA, the two-body operator does not follow from the equation for a free two-body t-matrix, but rather contains the mass of the nucleus (in which the two-body system is embedded) in the kinetic energy. Though this seems to be mathematically sound, such a two body t-matrix can have physically undesired features. For example, in [17] it was found from a phase shift study that such a two-body t-matrix may not display the resonant behaviour which it would be expected to. In the same work, in connection with π -nucleus scattering, it was found that considering a free two-body matrix simulated the contribution of continuum states (otherwise neglected in that work) and brought theory in closer agreement with data.

Though the differences arising from the particular approaches used above may not be crucial at the low energies considered in the present work, the many-body problem considered here is a bit more complicated and hence a small discussion is in order. In the works mentioned above, one studies the differences of the approaches involved, in a multiple scattering of a hadron on the individual nucleons in the nuclear target. Here however, the problem appears to be that of one multiple scattering problem embedded inside another. The η mesons scatter off the ^3He and ^4He nuclei as in a three body multiple scattering problem (of the η - ^3He - ^4He system). However, the individual η - ^3He and η - ^4He scatterings are represented by t-matrices for the multiple scatterings of the η on the three and four nucleons inside ^3He and ^4He . We choose then to work in a framework where we start by

evaluating the momenta k and k' in the η - ${}^7\text{Be}$ centre of mass frame and then evaluate the individual η - ${}^3\text{He}$ and η - ${}^4\text{He}$ t-matrices at a Lorentz boosted energy-momentum in the η - ${}^3\text{He}$ and η - ${}^4\text{He}$ centre of mass systems. The energy in the in-medium propagators (inside ${}^7\text{Be}$) is however taken to be in the η - ${}^7\text{Be}$ centre of mass system.

3. Cluster wave functions of ${}^6\text{Li}$ and ${}^7\text{Be}$

Since the energy spacing between the first four low-lying levels of the ${}^7\text{Be}$ nucleus is small, we include the contribution from these four levels. We consider the angular momentum states with $L = 1$ and $L = 3$ corresponding to the $J = (3/2^-, 1/2^-)$ and $J = (7/2^-, 5/2^-)$ levels respectively. The cluster wave functions for ${}^7\text{Be}$ and those for ${}^6\text{Li}$ required in the production amplitude of the $p + {}^6\text{Li} \rightarrow \eta + {}^7\text{Be}$ reaction are (1) generated using a Wood-Saxon potential [18] and (2) taken from a Green's function Monte Carlo (GFMC) variational calculation with the Urbana potential [19]. In the GFMC case, the wave function for ${}^7\text{Li}$ is used to represent the ${}^7\text{Be}$ one. The α and deuteron cluster in ${}^6\text{Li}$ is assumed to be in the $L = 0$ state.

B. Production mechanism of the $p + {}^6\text{Li} \rightarrow \eta + {}^7\text{Be}$ reaction

Assuming that the beam proton interacts with a loosely bound deuteron in the ${}^6\text{Li}$ nucleus to produce an η meson and ${}^3\text{He}$ (with the α remaining a spectator) the production amplitude for the $p + {}^6\text{Li} \rightarrow \eta + {}^7\text{Be}$ reaction can be written in terms of that for the $p + d \rightarrow {}^3\text{He} + \eta$ process. The off shell η meson thus produced then rescatters on ${}^7\text{Be}$ (i.e. the ${}^3\text{He}$ - ${}^4\text{He}$ cluster). This production of the η and its final state interaction (FSI) with ${}^7\text{Be}$ is represented schematically in Fig. 1, and the corresponding transition matrix is written as,

$$T = \langle \vec{k}_\eta, m_\eta | T_{p{}^6\text{Li} \rightarrow \eta{}^7\text{Be}} | \vec{k}_p; m_p, m_6 \rangle \quad (10)$$

$$+ \sum_{m'_\eta} \int \frac{d\vec{q}}{(2\pi)^3} \frac{\langle \vec{k}_\eta, m_\eta | T_{\eta{}^7\text{Be} \rightarrow \eta{}^7\text{Be}} | \vec{q}, m'_\eta \rangle}{E(k_\eta) - E(q) + i\epsilon} \langle \vec{q}, m'_\eta | T_{p{}^6\text{Li} \rightarrow \eta{}^7\text{Be}} | \vec{k}_p; m_p, m_6 \rangle$$

where \vec{k}_p and \vec{k}_η are the initial and final momenta in the centre of mass system. m_p, m_6 and m_η are the spin projections of the proton, ${}^6\text{Li}$ and ${}^7\text{Be}$ respectively. The production matrix

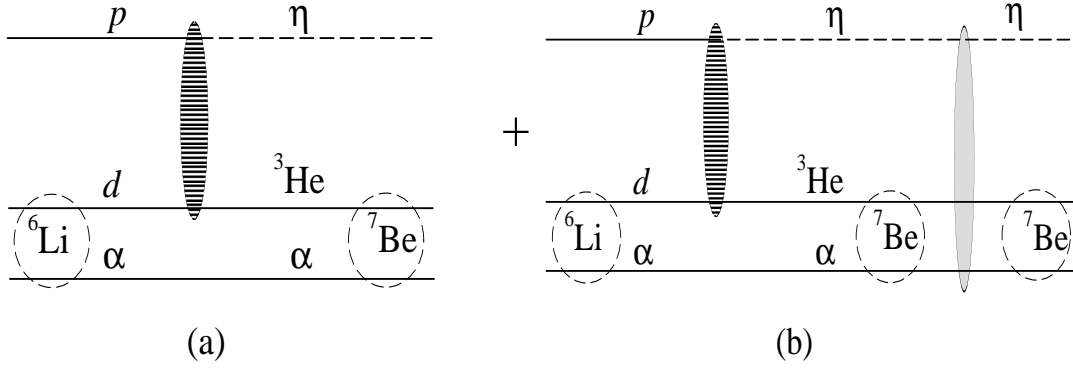


FIG. 1: Cluster model for η production in the $p + {}^6\text{Li} \rightarrow \eta + {}^7\text{Be}$ reaction. Diagram (a) corresponds to the direct on-shell η production and (b) to an η which is first produced off-shell and rescatters via the $\eta + {}^7\text{Be} \rightarrow \eta + {}^7\text{Be}$ process to become on-shell.

for a relative angular momentum L between the ${}^3\text{He}$ and α is written as,

$$\begin{aligned} \langle \vec{k}_\eta(\vec{q}), m'_7 | T_{p{}^6\text{Li} \rightarrow \eta{}^7\text{Be}} | \vec{k}_p; m_p, m_6 \rangle &= \frac{i}{(2\pi)^3} \frac{1}{\sqrt{4\pi}} \int P_1^2 dP_1 d\Omega_{P_1} \Psi_0^6(P_1) \\ &\sum_{M,\mu} \langle J, m'_7 | \frac{1}{2}, \mu, L, M \rangle \Psi_L^{*7}(P_2) Y_{LM}^*(\hat{P}_2) \\ &\times \langle \vec{k}_\eta(\vec{q}), \frac{-3}{7}\vec{k}_\eta(\vec{q}) + \vec{P}_2, \frac{1}{2}, \mu | T_{pd \rightarrow \eta{}^3\text{He}} | \frac{1}{2}, m_p, 1, m_6, \vec{k}_p, -\frac{1}{3}\vec{k}_p + \vec{P}_1 \rangle, \end{aligned} \quad (11)$$

where, \vec{k}_p is the momentum of the incoming proton and $-[2/6]\vec{k}_p + \vec{P}_1$ of the deuteron in ${}^6\text{Li}$. μ is the spin projection of ${}^3\text{He}$. The on-shell η meson momentum is denoted as \vec{k}_η and the off-shell one as \vec{q} . $[-3/7]\vec{k}_\eta + \vec{P}_2$ or $[-3/7]\vec{q} + \vec{P}_2$ is hence the momentum of on- or off-shell ${}^3\text{He}$ in ${}^7\text{Be}$. Since the α particle remains a spectator, its momentum in ${}^6\text{Li}$ and ${}^7\text{Be}$ is required to be the same and $-[4/6]\vec{k}_p - \vec{P}_1 = -[4/7]\vec{k}_\eta(\vec{q}) - \vec{P}_2$ (for on-shell (off-shell) η production). Thus $\vec{P}_2 = \vec{P}_1 + [2/3]\vec{k}_p - [4/7]\vec{k}_\eta(\vec{q})$ (where \vec{P}_1 and \vec{P}_2 are the Fermi momenta inside ${}^6\text{Li}$ and ${}^7\text{Be}$ respectively). The integration in (11) should in principle have been over both the Fermi momenta, \vec{P}_1 and \vec{P}_2 , however, the above relation between them renders the integration over \vec{P}_2 in (11) redundant. Further, when one evaluates the unpolarized cross sections, one sums over the spins in the final state and averages over those in the initial state. As a result, in such a calculation, some sums in (10) and (11) become redundant.

The T -matrix for the process, $\langle | T_{pd \rightarrow \eta{}^3\text{He}} | \rangle$, is written in a two-step model from our earlier work [6]. Considering the complexity of the present calculations which include the off-shell rescattering as given by the second term in (10) with the η - ${}^7\text{Be}$ FSI and the fact that the two-step model of the $p + d \rightarrow {}^3\text{He} + \eta$ is itself quite involved, we neglect the

effect of Fermi motion on $\langle |T_{pd \rightarrow \eta^3 He}| \rangle$ and hence take it out of the integral over P_1 in (11). The momentum space wave functions are expressed in terms of Fourier transforms of their radial forms. Thus the integral in momentum space is transformed to that in coordinate space. All this simplifies Eq. (11) to a good extent and it can be written as,

$$\begin{aligned} \langle \dots | T_{p^6 Li \rightarrow \eta^7 Be} | \dots \rangle &= i^{(L+1)} \sqrt{4\pi} \sum_{M\mu} Y_{LM}^*(\hat{Q}) F_L(Q) \langle J, m'_7 | \frac{1}{2}, \mu, L, M \rangle \\ &\times \langle \dots | T_{pd \rightarrow \eta^3 He} | \dots \rangle \end{aligned} \quad (12)$$

where,

$$F_L(Q) = \int_0^\infty r^2 dr \Psi_L^{*7}(r) j_L(Qr) \Psi_0^6(r) \quad (13)$$

is the transition form factor for ${}^6\text{Li} \rightarrow {}^7\text{Be}$, with momentum transfer $\vec{Q} = \frac{4}{7}\vec{q} - \frac{2}{3}\vec{k}_p$

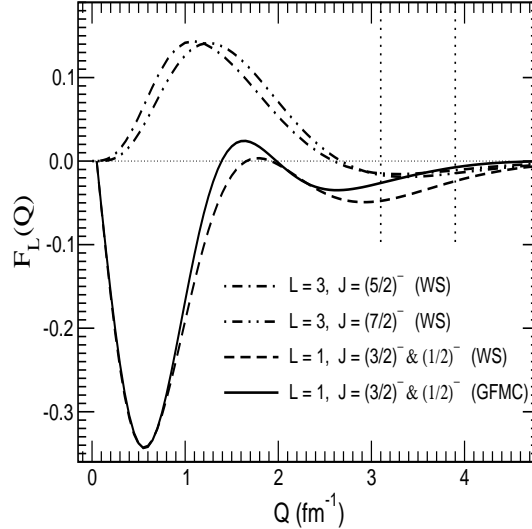


FIG. 2: The ${}^6\text{Li}$ - ${}^7\text{Be}$ transition form factor for angular momentum states with $L = 1$ and $L = 3$. The solid line corresponds to the GFMC variational wave functions with the Urbana potential for $L = 1$ and the dashed, dot-dashed and double dot-dashed lines are those generated using a Woods-Saxon potential (for $L = 1$ and $L = 3$).

for example in the off-shell case. Though not written explicitly, the transition form factor depends on the total angular momentum J since the radial wave function in ${}^7\text{Be}$ depends, even if mildly, on J . In Fig. 2 we present the two form factors with $L = 1$ ($J = 1/2^-$, $3/2^-$) and $L = 3$ ($J = 5/2^-$, $7/2^-$) required in the present work, using two different prescriptions of the nuclear wave functions mentioned in the previous section. With the $L = 1$ levels, $J = 1/2^-$ and $J = 3/2^-$ being very close to each other, the difference between the two

$L = 1$ form factors is not visible in the figure. The form factor enters (10) via (12) as (11) is simplified to (12) due to the neglect of the Fermi motion in the $p + d \rightarrow {}^3\text{He} + \eta$ t-matrix. It is evaluated at $\vec{Q} = \frac{4}{7}\vec{k}_\eta - \frac{2}{3}\vec{k}_p$ in the first term of (10) whereas over a range of momenta in the second term of (10) where it appears inside the integral. The dotted vertical lines in Fig. 2 indicate the relevant range corresponding to the beam energies of the present work. We shall see later how this difference between the two types of form factors affects the cross sections.

III. RESULTS AND DISCUSSIONS

In what follows, we shall present the cross section calculations for the $p + {}^6\text{Li} \rightarrow \eta + {}^7\text{Be}$ reaction with an emphasis on the η - ${}^7\text{Be}$ FSI. The transition matrices for the elementary processes $\pi + N \rightarrow \eta + N$ and $\eta + N \rightarrow \eta + N$ which enter as inputs to the production and FSI matrices are chosen from coupled channels calculations. The calculations in Figs 3-7 are done within Model A with a choice of parameters which corresponds to a scattering length of $a_{\eta N} = 0.88 + i0.41$ fm. Within the two-step model of the $p + d \rightarrow {}^3\text{He} + \eta$ reaction we use here, the data on this reaction were reproduced well with this choice of the scattering length.

In Fig. 8, a comparison of the total (inclusive) cross sections within models A and B of the $\eta N \rightarrow \eta N$ t-matrix and using different sets of scattering lengths is made.

A. The $p + {}^6\text{Li} \rightarrow \eta + {}^7\text{Be}$ cross sections for different ${}^7\text{Be}$ levels

As mentioned earlier, the $p + {}^6\text{Li} \rightarrow \eta + {}^7\text{Be}$ reaction is studied with four possible final states of the ${}^7\text{Be}$ nucleus. The proton beam energies are chosen to study the cross sections up to excess energies of about 20 MeV above threshold. Due to the differences between the masses of the various ${}^7\text{Be}$ levels, the threshold for the reaction corresponding to each level differs. In Table I, as an example, we list some of the beam energies at which we evaluate the cross sections, along with the corresponding excess energies in order to facilitate the understanding of the plots later.

In Figs 3 and 4, the angle integrated total cross sections for the $p + {}^6\text{Li} \rightarrow \eta + {}^7\text{Be}$ reaction are shown as a function of the proton beam energy. The dashed lines are the cross

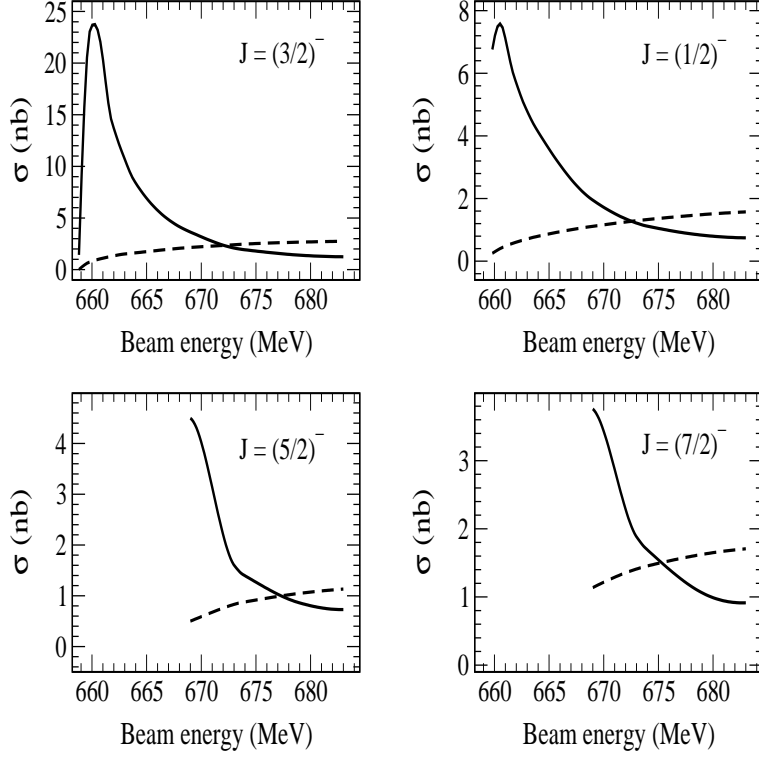


FIG. 3: Total cross sections as a function of the proton beam energy for different states of the ${}^7\text{Be}$ nucleus. The dashed lines are plots without the inclusion of the η - ${}^7\text{Be}$ final state interaction. The wave functions for ${}^6\text{Li}$ and ${}^7\text{Be}$ are generated using the Woods-Saxon potential.

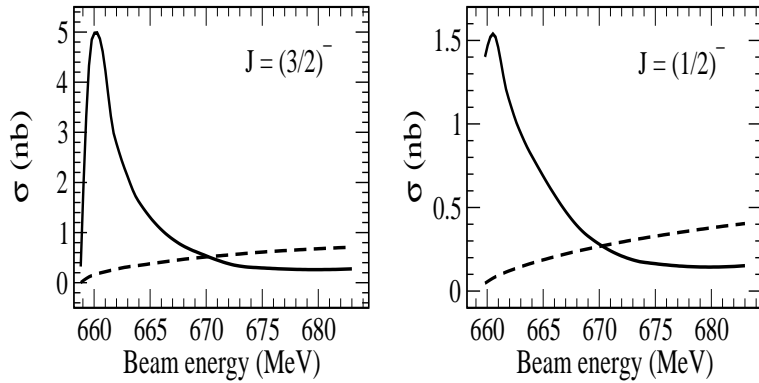


FIG. 4: Same as Fig. 3 except for the fact that the wave functions for ${}^6\text{Li}$ and ${}^7\text{Be}$ are from the GFMC variational method with the Urbana potential.

sections evaluated using only Fig. 1(a) corresponding to the first term in Eq. (10). As is evident from these plots, inclusion of Fig. 1(b), i.e., the rescattering of the η meson with the ${}^7\text{Be}$ nucleus (or in other words the final state η - ${}^7\text{Be}$ interaction) drastically affects the

TABLE I: Beam and excess energies for different levels of the ${}^7\text{Be}$ nucleus

Beam energy (MeV)	Excess energy = $E_{\eta-{}^7\text{Be}} - M_{{}^7\text{Be}} - M_{\eta}$ (MeV)			
	L = 1		L = 3	
	J = (3/2) ⁻ ground state	J = (1/2) ⁻	J = (7/2) ⁻	J = (5/2) ⁻
658.8	0.0003	-	-	-
659.8	0.791	0.361	-	-
663.8	3.954	3.524	-	-
669	8.056	7.626	3.426	1.376
673.8	11.855	11.425	7.225	5.175
683	19.11	18.679	14.478	12.428

shape and magnitude of the cross sections near threshold.

1. The off-shell rescattering contribution

The second term in Eq. (10) which corresponds to rescattering (Fig. 1(b)), consists in principle of the scattering of on- as well as off-shell η mesons on ${}^7\text{Be}$. As is generally expected at low energies, Fig. 5 clearly shows that neither the plane wave scattering (Fig. 1a) nor the pole term in Eq. (10) (the on-shell η - ${}^7\text{Be}$ rescattering) is responsible for the near threshold cross section hump. It is the principal value of the integral in the second term which corresponds to the scattering of off-shell eta mesons produced in the $p + {}^6\text{Li} \rightarrow \eta + {}^7\text{Be}$ process on ${}^7\text{Be}$ that gives rise to this hump. Though the dominance of the principal value is expected, a hump-like structure in the total cross section, due to final state η -nucleus interaction is not so natural to expect. For example, such an effect was not observed in our previous studies of the $pd \rightarrow pd\eta$ and $pd \rightarrow {}^3\text{He} \eta$ reactions.

In order to understand this phenomenon, we re-write the principal value integral in the second term of Eq. (10) (corresponding to off-shell rescattering) in a split form. Let us express the integral $\int d\vec{q} = \int d\Omega_q \int_0^\infty q^2 dq$ as $\int d\Omega_q \int q \mu dE(q)$ where, $q^2 = 2\mu E(q)$. Dropping the spin projection dependence in the notation for convenience, we define the

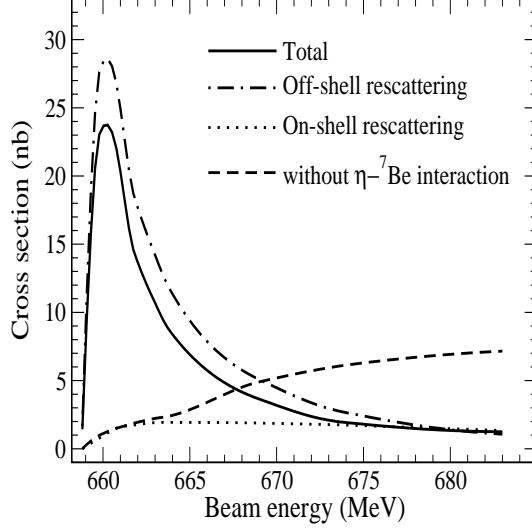


FIG. 5: Contributions of the plane wave (dashed line), on-shell rescattering (dotted line) and off-shell rescattering (dot-dashed line) terms to the total cross section (solid line) for the $p + {}^6\text{Li} \rightarrow \eta + {}^7\text{Be}$ reaction with ${}^7\text{Be}$ in its ground state ($J = 3/2^-$). The cluster model nuclear wave functions are generated using the Woods-Saxon potential.

rescattering term alone (second term in (10)) as a function, $G(\vec{k}_p, \vec{k}_\eta)$ plus the pole term, such that,

$$\int \frac{d\vec{q}}{(2\pi)^3} \frac{\langle \vec{k}_\eta | T_{\eta {}^7\text{Be}} | \vec{q} \rangle}{E(k_\eta) - E(q) + i\epsilon} \langle \vec{q} | T_{p {}^6\text{Li} \rightarrow \eta {}^7\text{Be}} | \vec{k}_p \rangle \quad (14)$$

$$= \mathcal{P} \int d\Omega_q F(\vec{k}_p, \vec{k}_\eta, \hat{q}) \int dE(q) \frac{f(E(q))}{E(k_\eta) - E(q)} + \text{pole term},$$

where the functions, F and f summarize the angle and energy dependence (except the energy dependence in the denominator) respectively of the vector \vec{q} in the integrand. We now break up part of the principal value integral into three parts, considering the region till and after the pole value as follows:

$$I = \int_0^{E(k_\eta) - \delta} \frac{f(E(q))}{E(k_\eta) - E(q)} dE(q) + \int_{E(k_\eta) + \delta}^{2E(k_\eta)} \frac{f(E(q))}{E(k_\eta) - E(q)} dE(q) \quad (15)$$

$$+ \int_{2E(k_\eta)}^\infty \frac{f(E(q))}{E(k_\eta) - E(q)} dE(q) = I_1 + I_2 + I_3.$$

In order to get some idea of the behaviour of the complicated integrals in (14) and (15) which we perform numerically, we try to analyse these integrals analytically in a very simplistic way. First, we perform an expansion of $f(E(q))$, such that,

$$f(E(q)) \simeq f(E(k_\eta)) + (E(k_\eta) - E(q)) f'(E(k_\eta)) + \dots$$

and hence,

$$\frac{f(E(q))}{E(k_\eta) - E(q)} \simeq \frac{f(E(k_\eta))}{E(k_\eta) - E(q)} + f'(E(k_\eta)) + \dots$$

We further assume that only the first term on the right in the above expansion is important. Not always can one expect the energy dependence of $f(E(q))$ to be such that we can write it with only a constant $f(E(k_\eta))$ appearing in the first term as above. If the pole is however close to zero, then the energy region $0 \rightarrow 2E(k_\eta)$ is a small region around the pole where $f(E(q))$ may vary little and the expansion made above becomes a reasonable approximation. Since $f(E(k_\eta))$ is a constant, when we integrate, we get,

$$I = \ln(E(k_\eta) - E(q)) \Big|_0^{E(k_\eta)-\delta} + \ln(E(k_\eta) - E(q)) \Big|_{E(k_\eta)+\delta}^{2E(k_\eta)} + I_3, \quad (16)$$

where obviously the first two terms cancel. The integral I in (15) will then be dominated only by I_3 whose behaviour will decide the shape of the off-shell rescattering term. I_3 depends on the form of the function $f(E(q))$, which is a product of the $p + {}^6\text{Li} \rightarrow \eta + {}^7\text{Be}$ production t-matrix and the η - ${}^7\text{Be}$ elastic t-matrix. The latter is peaked at small k_η due to the fact that the ${}^7\text{Be}$ wave function contributes at large r . The I_3 part of the off-shell rescattering term which grows as one approaches energies close to threshold gives rise to the hump due to FSI in the total cross section. The above analysis will not be valid when one is far away from threshold.

2. Single scattering versus multiple scattering to all orders

In Fig. 6, for the sake of completeness is shown the cross section evaluated using only the single scattering terms in the η - ${}^7\text{Be}$ t-matrix (i.e. the first terms in Eqs (4 - 5)) as compared to that using the full coupled channel t-matrix which includes the multiple scattering to all orders (Eqs (4- 6)). The dot-dashed line is thus the calculation corresponding to an η - ${}^7\text{Be}$ interaction where the η meson scatters once on each of the ${}^3\text{He}$ and ${}^4\text{He}$ nuclei inside ${}^7\text{Be}$ and then proceeds to become on-shell in the final state of the $p + {}^6\text{Li} \rightarrow \eta + {}^7\text{Be}$ reaction. The solid line is due to the η - ${}^7\text{Be}$ interaction which involves multiple scattering of the η on the two clusters, ${}^3\text{He}$ and ${}^4\text{He}$, and its propagation inside ${}^7\text{Be}$ in between these scatterings.

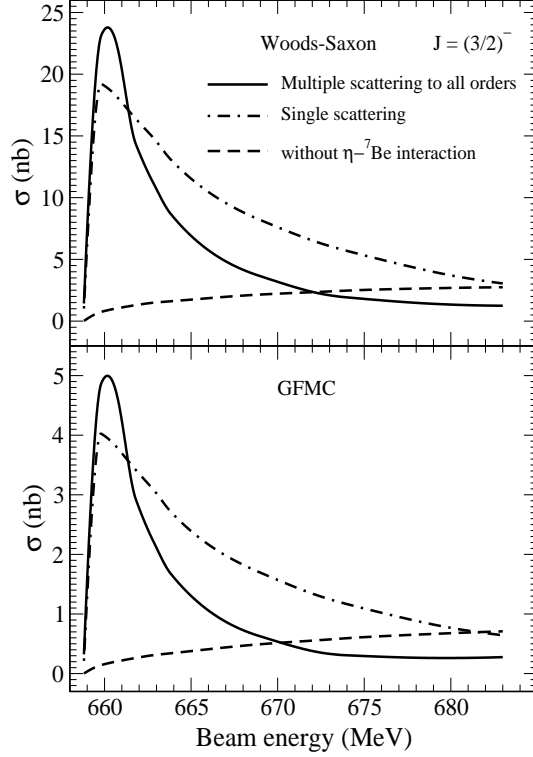


FIG. 6: Total cross sections evaluated using only the single scattering term (dot-dashed) in the η - ${}^7\text{Be}$ interaction, the full calculation (solid line) involving η meson rescattering and propagation inside ${}^7\text{Be}$ to all orders and the one without the inclusion of the η - ${}^7\text{Be}$ interaction (dashed line). The calculation is done for the ground state of ${}^7\text{Be}$ ($J = 3/2^-$).

3. Angular distributions

In Fig. 7, we plot the angular distributions for this reaction for the ground state ($J = 3/2^-$) of ${}^7\text{Be}$. The angular distributions are nearly isotropic as has always been found in the η producing reactions near threshold. The FSI between the η meson and ${}^7\text{Be}$ is responsible for raising the magnitudes of the cross sections only close to threshold. At an excess energy of 19 MeV, the effect of the FSI is highly reduced and the theoretical prediction in Fig. 7 is around 0.2 nb/sr as compared to the Turin data point of 4.6 ± 3.8 nb/sr. Even if we add up the cross sections corresponding to other values of J , i.e., $J = 1/2^-$, $5/2^-$ and $7/2^-$, the theoretical prediction with FSI is 0.51 nb/sr. Though not very clear at the moment, one could speculate that the deficit in the theoretical prediction as compared to data is probably due to some missing reaction mechanism not included in the present cluster model approach.

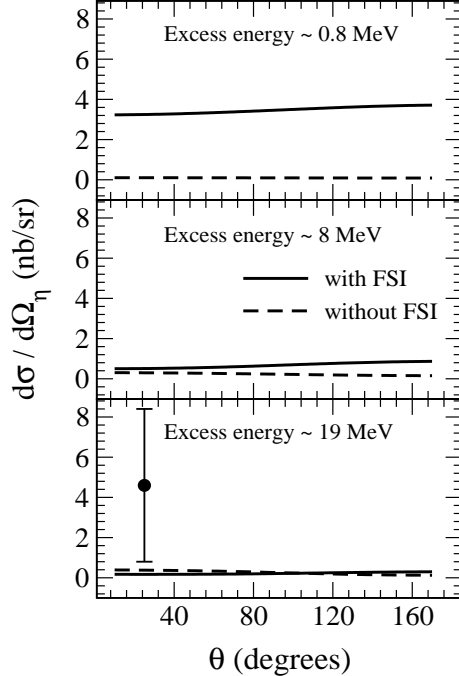


FIG. 7: Angular distributions for the $p + {}^6\text{Li} \rightarrow \eta + {}^7\text{Be}$ reaction at different excess energies (corresponding to different beam energies). The data point is by the Turin group [7]. Solid and dashed lines correspond to the calculations with and without the inclusion of the η - ${}^7\text{Be}$ interaction respectively. The calculation is done for the ${}^7\text{Be}$ ground state and using Woods-Saxon wave functions.

B. Inclusive cross section

Having analysed and deciphered the origin of the hump in the total cross sections near threshold, we now plot in Fig. 8, the sum of the total cross sections, $\sum_J \sigma_{p+{}^6\text{Li} \rightarrow \eta + {}^7\text{Be}}^J$, where the superscript J refers to the state in which the ${}^7\text{Be}$ in the final state is produced. The four different levels of ${}^7\text{Be}$ considered here have a different value of J and also a different mass. In this sense, the summed cross section represents an inclusive cross section of the $p + {}^6\text{Li} \rightarrow \eta + X$ reaction with X being any of the low-lying states of ${}^7\text{Be}$. We have already seen that within Model A, the close to threshold η - ${}^7\text{Be}$ interaction causes a sharp rise (the hump) in the cross section. Now, in the case of the $L = 3$ states, as can be seen from Table I, the threshold is shifted by about 10 MeV as compared to the $L = 1$ states. As a result, the $L = 3$ humps appear and contribute at a higher beam energy. Since the hump is a close to threshold phenomenon, the $L = 1$ cross sections already fall down a lot before the $L = 3$

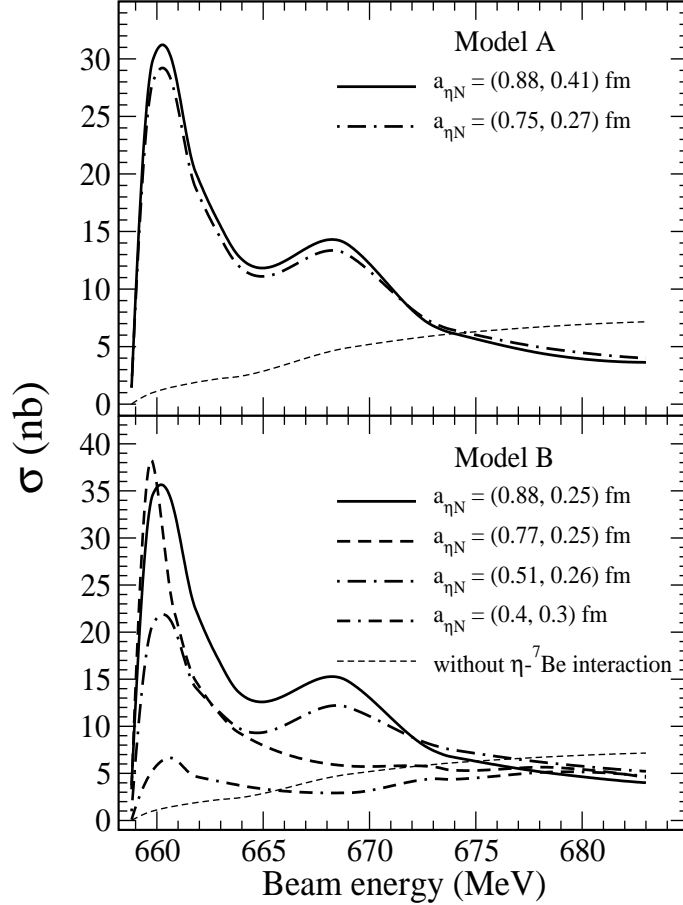


FIG. 8: Total cross sections for the inclusive reaction $p + {}^6\text{Li} \rightarrow \eta + {}^7\text{Be}$. Inclusive implies that the cross section for four J values of ${}^7\text{Be}$, namely, $1/2^-$, $3/2^-$, $5/2^-$ and $7/2^-$ have been summed. The upper and lower panel display results within two different models of the ηN interaction used for evaluating the η - ${}^7\text{Be}$ FSI as described in the text. The dotted line without any humps corresponds to the calculation without the η - ${}^7\text{Be}$ final state interaction.

humps begin. The result is a double hump structure in the inclusive $p + {}^6\text{Li} \rightarrow \eta + {}^7\text{Be}$ reaction.

The cross sections evaluated in Model B, have a similar form as those in Model A except for two values of the scattering lengths, namely, $(0.77, 0.25)$ fm and $(0.4, 0.3)$ fm. For these two values, the cross sections do not display a very prominent second hump. After a careful reading of Ref. [14] (which lists the parameter sets for Model B, lower panel in Fig. 8) one notices that the parameter sets for these two particular curves have been obtained after removing the $\gamma N \rightarrow \eta N$ data from the analysis. Thus these two curves are different from all the rest in Fig. 8, in the sense that these parameter sets are not constrained by the

photoproduction data. Model A, however, was used in [13] to calculate the cross sections for the $\gamma d \rightarrow \eta d$ and $\gamma d \rightarrow \eta X$ reactions. Hence, Model A and the two curves with double humps in Model B are constrained by the eta photoproduction data which is probably important for the behaviour of the ηN t -matrix at energies away from threshold.

C. Comment on possible eta-mesic ${}^7\text{Be}$ states

Finally, before ending our discussion of the results, in Table II, we give the η - ${}^7\text{Be}$ scattering lengths corresponding to different values of the ηN scattering lengths in models A and B. The η - ${}^7\text{Be}$ scattering length is evaluated from the elastic η - ${}^7\text{Be}$ t -matrix at zero energy as follows:

$$a_{\eta-{}^7\text{Be}} = - \frac{\mu T_{\eta-{}^7\text{Be}}(0, 0, 0)}{2\pi}, \quad (17)$$

where μ is the reduced mass of the η - ${}^7\text{Be}$ system. The smallest scattering length $a_{\eta N}$ used

TABLE II: η - ${}^7\text{Be}$ scattering lengths, $a_{\eta-{}^7\text{Be}}$, for the ground state of ${}^7\text{Be}$, corresponding to different values of $a_{\eta N}$.

	$a_{\eta N}$ (fm)	$a_{\eta-{}^7\text{Be}}$ (fm)
Model A	$0.75 + i0.27$	$-10.09 + i8.19$
	$0.88 + i0.41$	$-9.18 + i8.53$
Model B	$0.88 + i0.25$	$-20.43 + i5.43$
	$0.77 + i0.25$	$-14.52 + i14.77$
	$0.51 + i0.26$	$-2.03 + i11.29$
	$0.4 + i0.3$	$0.29 + i6.43$

here, leads to a positive real part of the η - ${}^7\text{Be}$ scattering length, $a_{\eta-{}^7\text{Be}}$. However, this choice of parameters (model F in [14]) is mentioned as an unconventional solution obtained after dropping the photoproduction data from the fits.

The first four entries in Table II corresponding to large $a_{\eta N}$, display $a_{\eta-{}^7\text{Be}}$ to be large with negative real parts. Apart from the commonly known condition that the real part of the scattering length should be negative [20], in the third reference in [2], the authors found that the condition for the existence of a bound state is that $|a_I| < |a_R|$ for an eta-nucleus

scattering length of $(a_R + i a_I)$. With these two conditions it seems that the first few entries in Table II for the large ηN scattering lengths support the possibility of eta-mesic states. In [21], while investigating the connection between the η - ^3He scattering lengths and the corresponding binding energies and widths, the authors also use the above conditions but mention that in reality none of the above can be taken as a sufficient condition. The bottomline is then that it would indeed be premature to base the conclusions only on the signs or magnitudes of the scattering lengths. One should rather perform a better analysis for the search of η - ^7Be states using the present η - ^7Be model and a time delay analysis as in [3, 22] or a K-matrix analysis as in [23] before drawing definite conclusions.

IV. SUMMARY

The present work aimed at performing a thorough investigation of the effects of the η - ^7Be interaction in the $p + ^6\text{Li} \rightarrow \eta + ^7\text{Be}$ reaction near threshold. The work was partly motivated by the recent revival of interest in this reaction by the COSY-GEM collaboration [9] after the first measurement in 1993. This work also comes as a sequel to our various earlier studies on η meson production in light nuclei. A two-step model for the $p + d \rightarrow ^3\text{He} + \eta$ reaction including the η - ^3He interaction was tested earlier with data by the present authors [6]. This model is used as an input to develop a cluster model approach for the $p + ^6\text{Li} \rightarrow \eta + ^7\text{Be}$ reaction near threshold. The η - ^7Be interaction is included in a multiple scattering formalism for an η scattering on a ^3He - ^4He cluster inside ^7Be . The η - ^3He and η - ^4He scatterings are themselves included using few body equations. The calculations are done for four low-lying levels of ^7Be . To the best of our knowledge, this is the most detailed study of the η - ^7Be interaction in the $p + ^6\text{Li} \rightarrow \eta + ^7\text{Be}$ reaction performed so far. The interesting two hump structure in the summed total cross section (summed over J) hints toward a very strong near threshold effect of the η - ^7Be interaction (especially of the off-shell rescattering of the η on ^7Be) which is worth verifying experimentally in future.

ACKNOWLEDGEMENTS

The authors gratefully acknowledge V. Jha for the help in computing the cluster wave functions using the Woods-Saxon potential and K. P. Khemchandani for her help with the $pd \rightarrow \eta$ - ^3He programs and many useful discussions. The authors are also thankful to the

anonymous referee for his/her constructive criticism. The work done by two of the authors, NJU and BKJ, was supported by the Ramanna fellowship, awarded by the Department of Science and Technology, Government of India, to BKJ.

- [1] M. Pfeiffer *et al.*, Phys. Rev. Lett. **92**, 252001 (2004); G. A. Sokol *et al.*, Part. Nucl. Lett. **102**, 71 (2000).
- [2] R. S. Bhalerao and L. C. Liu, Phys. Rev. Lett. **54** (1985) 865; L.C. Liu and Q. Haider, Phys. Rev. C **34**, 1845 (1986); Q. Haider and L.C. Liu, Phys. Rev. C **66**, 045208 (2002).
- [3] N. G. Kelkar, K. P. Khemchandani and B. K. Jain, J. Phys. G:Nucl. Part. Phys. **32**, L19 (2006); N. G. Kelkar, K. P. Khemchandani and B. K. Jain, J. Phys. **G 32**, 1157 (2006); N. G. Kelkar, Phys. Rev. Lett. **99**, 210403 (2007).
- [4] S. Wycech, Anthony M. Green and J.A. Niskanen, Phys. Rev. **C 52**, 544 (1995); V.A. Tryasuchev, Phys. Atom. Nucl. **60**, 186 (1997) (Yad. Fiz. **60**, 245 (1997)); C.Y. Song, X.H. Zhong and L. Li, P.Z. Ning, Europhys. Lett. **81**, 42002 (2008); D. Jido, E.E. Kolomeitsev, H. Nagahiro and S. Hirenzaki, Nucl. Phys. **A 811**, 158 (2008); H. Nagahiro, D. Jido and S. Hirenzaki, arXiv:0811.4516.
- [5] J. Berger *et al.*, Phys. Rev. Lett. **61**, 919 (1988); B. Mayer *et al.*, Phys. Rev. C **53**, 2068 (1996); A. Wrońska *et al.*, Int. J. Mod. Phys. A **20**, 640 (2005); H., -H., Adam *et al.*, Phys. Rev. C **75**, 014004 (2007).
- [6] K.P. Khemchandani, N.G. Kelkar and B.K. Jain, Nucl. Phys. **A 708**, 312 (2002); *ibid*, Phys. Rev. C **68**, 064610 (2003); N.J. Upadhyay, K.P. Khemchandani, B.K. Jain and N.G. Kelkar, Phys. Rev. C **75**, 054002 (2007); K. P. Khemchandani, N. G. Kelkar and B. K. Jain, Phys. Rev. C **76**, 069801 (2007).
- [7] Scomparin E. *et al.*, J. Phys. G: Nucl. Part. Phys. **19** L 51, (1993).
- [8] J. S. Al-Khalili, M. B. Barbaro and C. Wilkin, J. Phys. G **19**, 403 (1993).
- [9] M. Ulicny *et al.*, AIP Conf. Proc. **603**, 543 (2001); H. Machner, Acta Phys. Slov. **56**, 227 (2006); e-Print: nucl-ex/0511034.
- [10] T. Kajino, T. Matsuse and A. Arima, Nucl. Phys. A **413**, 323 (1984).
- [11] J. V. Noble, Phys. Rev. C **9**, 1209 (1974); A. C. Merchant and N. Rowley, Phys. Lett. B **150**,

- 35 (1985).
- [12] S. A. Rakityansky *et al.*, Phys. Rev. C **53**, 2043 (1996); S. A. Rakityansky *et al.*, Few Body Syst. Suppl. **9**, 227 (1995).
 - [13] A. Fix and H. Arenhövel, Eur. Phys. J A **9**, 119 (2000).
 - [14] A. M. Green and S. Wycech, Phys. Rev. C **71**, 014001 (2005).
 - [15] E. Kujawski and E. Lambert, Annals of Physics **81**, 591 (1973).
 - [16] R. Crespo, A. M. Moro and I. J. Thompson, Nucl. Phys. A **771**, 26 (2006).
 - [17] V. B. Belyaev, S. A. Rakityansky and J. Wrzcionko, Nucl. Phys. A **368**, 394 (1981).
 - [18] B. Buck and A. C. Merchant, J. Phys. G **14** L211 (1988); V. I. Kukulin, V. G. Neudatchin and Yu. F. Smirnov, Nucl. Phys. A **245** (1975) 429.
 - [19] J. L. Forest *et al.*, Phys. Rev. C **54**, 646 (1996).
 - [20] C. J. Joachain 1975 *Quantum Collision Theory* (North-Holland), p.288.
 - [21] A. Sibirtsev, J. Haidenbauer, J. A. Niskanen and Ulf-G. Meissner, Phys. Rev. C **70**, 047001 (2004); see also J. A. Niskanen, arXiv: nucl-th/0508021.
 - [22] N. G. Kelkar, M. Nowakowski, K. P. Khemchandani and S. R. Jain, Nucl. Phys. **A730**, 121 (2004); N. G. Kelkar, M. Nowakowski and K. P. Khemchandani, Nucl. Phys. **A724**, 357 (2003); *ibid*, Mod. Phys. Lett. A **19**, 2001 (2004).
 - [23] S. Wycech and A. M. Green, Int. J. Mod. Phys. A **20**, 637 (2005).